Available online at www.sciencedirect.com
ScienceDirect
Acta Materialia 57 (2009) 4539–4547
Acta MATERIALIA
www.elsevier.com/locate/actamat

# Abnormal grain growth in Al–3.5Cu

J. Dennis, P.S. Bate *, F.J. Humphreys

*School of Materials, University of Manchester, Manchester M1 7HS, UK*

Received 13 May 2009; accepted 14 June 2009
Available online 14 July 2009

**Abstract**

Significant abnormal grain growth has been observed in an Al–3.5 wt.% Cu alloy at temperatures where the volume fraction of small $CuAl_2$ particles was less than about 0.01. The initial fine-grained material had a weak crystallographic texture and there was no indication that any special boundaries were involved in the abnormal growth. Island grains isolated within the abnormal grains also showed no indication of special orientation relationships with their surrounding grains. Measurements indicated that the island grains initially had a size advantage over other matrix grains. The fraction of pinning phase was much lower at abnormal grain boundaries than at boundaries in the fine-grained matrix into which they were growing. A variety of simulations were made, including attempts to model that difference in pinning phase distribution, but none of these were successful in predicting abnormal grain growth.


*Keywords:* Abnormal grain growth; Secondary recrystallization; Aluminium

## 1. Introduction

Grain growth is a very familiar annealing phenomenon in which the increase in mean grain size with time is driven by the reduction in grain boundary surface area, and takes place via diffusion-controlled processes at the grain boundaries. In many cases, the distribution of grain sizes remains similar at different stages of growth, i.e. the probability distribution in terms of the logarithm of grain size simply shifts as growth proceeds. However, in some cases a small population of grains grows at a significantly faster rate than the other, "matrix", grains; these grains become abnormally large and the process is referred to as abnormal grain growth.

In some respects, this discontinuous (in terms of the size distribution) behaviour is similar to the typical recrystallization process, and has been referred to as secondary recrystallization. This terminology was used by Dunn and Walter [1] in their review, over 40 years ago, of the phenomenon. They identified three main factors of importance: the effect of orientation on boundary mobility, the influence of second-phase particles, and the interactions of boundaries with specimen surfaces. For present purposes, the last of those can be ignored. Orientation effects have received a good deal of attention, primarily because of the technological importance of the development of the strong Goss $\{0\,1\,1\}\ \langle 1\,0\,0\rangle$ texture in Fe–Si sheets, used in electrical transformer cores, by abnormal grain growth. There have been a number of reports of abnormal grain growth in materials with strong (primary) recrystallization textures, sometimes in the absence of second-phase particles, and even when the effects of particles are likely to be important, the potential effects of grain boundary misorientation have been assumed to be dominant.

It is generally accepted that second-phase particles have an important effect on the occurrence of abnormal grain growth [1,2]. Second-phase particles lead to grain boundary pinning via the well-known Zener mechanism, which halts grain growth. In almost all cases of abnormal grain growth, a microstructure of Zener-pinned grains is destabilized by dissolution of the pinning phase. There have been analyses of that situation using analytical and statistical, or "mean field", models. Hillert [3] emphasized the role of particle dissolution, and suggested that abnormal growth

* Corresponding author. Address: School of Materials, University of Manchester, Grosvenor Street, Manchester M1 7HS, UK.
*E-mail address:* pete.bate@manchester.ac.uk (P.S. Bate).

1359-6454/$36.00 © 2009 Acta Materialia Inc. Published by Elsevier Ltd. All rights reserved.
doi:10.1016/j.actamat.2009.06.018

would occur when a single large grain, or a small number of distributed large grains, existed in a matrix with a grain size between two limits determined by the Zener pinning. Essentially the same general conclusions were reached in the analyses of Andersen et al. [4] and Humphreys [5], and in a number of subsequent investigations.

However, although the statistical models appear to give reasonable results, there has been a lack of success when attempting to simulate abnormal grain growth using spatially resolved models, i.e. those that aim to explicitly represent the microstructure; at least when significant grain boundary anisotropy is not present. The most significant model in this context is the Monte Carlo–Potts (MCP) type, although two-dimensional vertex modelling has been used with the same conclusion that unless there is significant boundary anisotropy, abnormal growth is not predicted [6]. When boundary anisotropy is present, MCP models can give abnormal growth (e.g. [7]). There is, though, a discrepancy between the "mean field" and the spatially resolved models when boundary anisotropy is not important. In that context, work on a material with a weak crystallographic texture is warranted, and is reported here.

## 2. Experimental

The initial phase of the experimental programme was focused on producing a material with a microstructure comprising small equiaxed grains and a uniform spatial distribution of near-spherical particles. Such a material would have advantages in terms of comparison with numerical models and other analyses compared to materials with more complex, heterogeneous, microstructures. The microstructures throughout this work were examined using optical metallography and, more significantly, by scanning electron microscopy (SEM) with orientation determination by electron backscatter diffraction (EBSD). Optical metallography used mechanically polished specimens which were anodized, using an aqueous solution of 5 vol.% $HBF_4$ with a small addition of $HBO_3$, at 20 V. The anodized surfaces were imaged using polarized light. Scanning electron microscopy used electropolished sections. The microscopes used were a Philips XL with a field emission gun (FEG), operated at potentials from 8 to 20 kV, and a CamScan MX250 FEGSEM. EBSD used equipment and software by HKL Technology as well as in-house software. Crystallographic texture was determined using EBSD data, again using in-house software.

### 2.1. Material preparation

A single Al–Cu alloy was used. This was produced using high-purity components and contained 3.46 wt.% Cu. Apart from a Zn content of 0.013 wt.%, all other impurity elements were at levels of $\leqslant$0.001 wt.%. The alloy was supplied by Alcan International Banbury Laboratories in the form of a direct chill cast 90 mm diameter cylinder. This was homogenized by heating to 500 °C for 2 h followed by soaking at 550 °C for 4 h, after which the material was water quenched. This gave reasonable compositional homogeneity and a grain size of about 0.4 mm. The water-quenched material was heat treated at 200 °C for 3 h followed by holding at 400 °C for 3 h. This gave a distribution of equilibrium $\theta$ $CuAl_2$ particles which was sufficiently uniform, and not dominated by large grain boundary precipitates.

In addition to a uniform particle distribution, a weak texture was desired. A range of deformation routes was investigated, and equal-channel angular extrusion (ECAE) preceded by flat rolling was chosen as the preferred route. The ECAE used a 15 mm square section billet taken from material cold rolled to a 50% thickness reduction. Eight ECAE passes were used, nominally at room temperature, with a 120° die and no billet rotation between passes. This material was annealed at 400 °C for 1 h. Following annealing, this process route gave the microstructure shown in Fig. 1. The grains were close to equiaxed, with a mean linear intercept size of 8.2 μm. The deformation and annealing spheroidized the $\theta$ particles, which had a mean diameter of 0.43 μm.

### 2.2. Annealed microstructures

The processed material was subject to annealing treatments at temperatures in the range 450–500 °C. Examples of microstructures after annealing are shown in Fig. 2. At temperatures below about 470 °C, gradual uniform grain growth occurred. At 500 °C, where the material is single phase, the grain size is much larger but the size distribution was typical of normal growth. At temperatures of 475 and 485 °C, abnormal grain growth occurred with significant bimodality in the grain size distribution. The evolution of grain size distribution at 465 and 485 °C is shown in

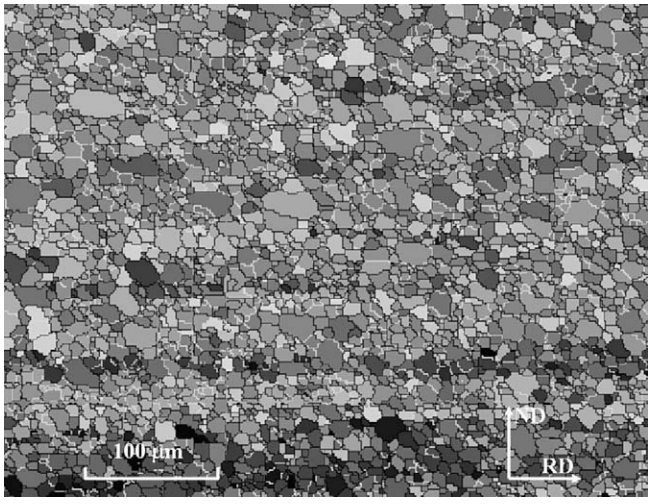


Fig. 1. SEM/EBSD orientation image of the microstructure of the Al–Cu alloy following ECAE processing and annealing at 400 °C for 1 h. The relationship between the grey scale and orientation is arbitrary.

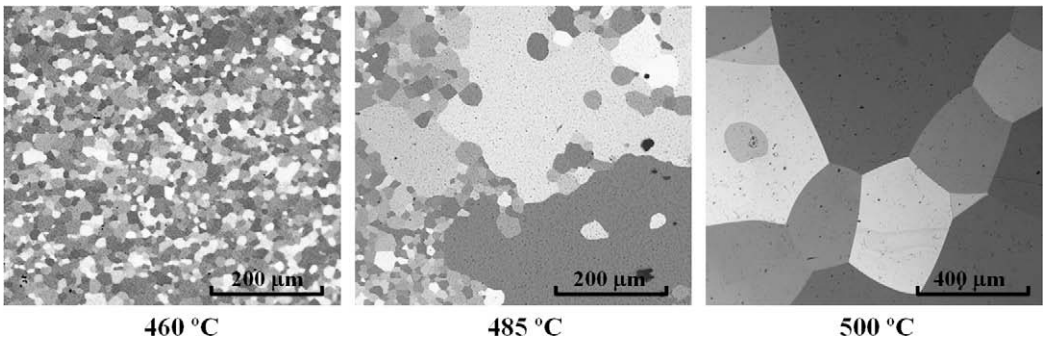


Fig. 2. Optical micrographs of anodized sections from material annealed at the temperatures indicated for 30 min. Abnormal growth has occurred at 485 °C, and island grains are visible in the abnormally large grains.

Fig. 3, from which the development of bimodality at the higher temperature is clear. Because there are relatively few abnormal grains, the bimodality is not apparent if grain number statistics are used, and the plots use areal probability density. This gives the probability density of a random point in a section of microstructure being within a grain of a given circular equivalent diameter. Probability densities were derived from discrete data using kernel density estimation, with an Epanichenikov kernel and adaptive bandwidth setting [8].

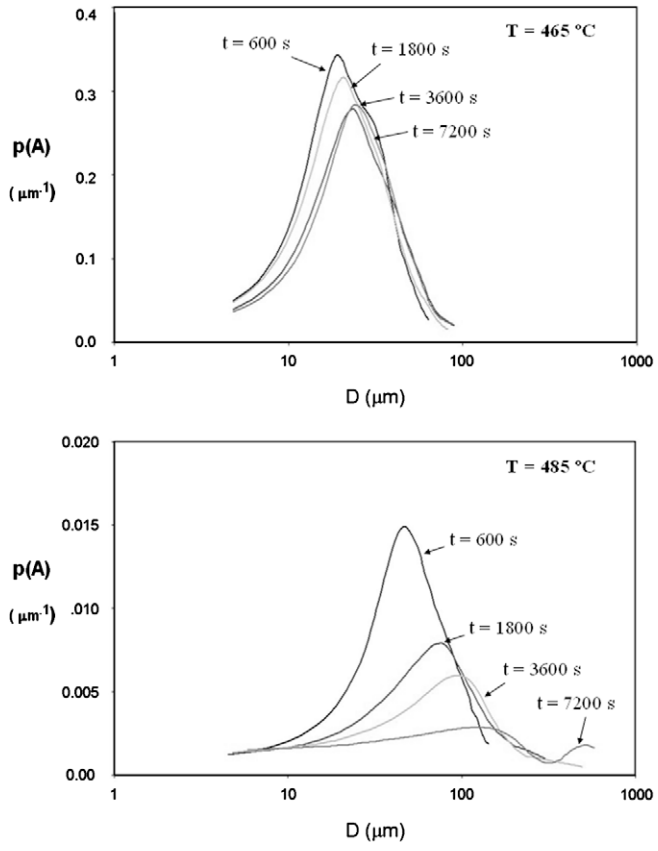


Fig. 3. Grain size distributions, as probability densities of grain area, for material annealed at the temperatures indicated for different times. Very little growth has taken place at 465 °C, but at 485 °C there is significant growth of the fine-grained matrix and the occurrence of a secondary peak in the distributions associated with the abnormally large grains.

A feature of the microstructures obtained here, and found previously, containing abnormally large grains is the occurrence of "island" grains, isolated within the abnormal grains. Examples can be seen in Fig. 2, which also shows "peninsular" grain groups. Serial sectioning showed that "island" grains were, generally, truly isolated.

The fundamental change that occurs with increasing temperature in this alloy is a reduction in the second-phase fraction. The measured volume fraction of $\theta$ $CuAl_2$ decreased with temperature. At 465 °C the volume fraction was 0.015 and at 485 °C it was 0.004. Extrapolation indicated complete dissolution at temperatures above 491 °C. The particle volume fraction changes very quickly to its "equilibrium" value during heat treatment, but particle coarsening also occurred. Particle size distributions after different annealing times at temperatures of 465 and 485 °C are shown in Fig. 4. In detail, the distribution of particles was not homogeneous, however, and there were some potentially important aspects of the distribution of particles with respect to the grain structures. These will be dealt with below.

### 2.3. Orientation relationships

In view of previous work, the orientation relationships and the misorientations associated with different grain boundary types are of interest. Continuous orientation density functions were obtained from individual orientation measurements using harmonic series [9], with a truncation level of $l_{max} = 22$. Monoclinic specimen symmetry was assumed, reflecting the deformation produced by ECAE.

The crystallographic texture of the initial microstructure, i.e. as annealed at 400 °C, from a sample of >2000 individual EBSD orientations, with no imposed Gaussian smoothing, is shown as a direct 0 0 1 pole figure in Fig. 5a. This texture was weak; the maximum orientation density of the orientation distribution function was only $f(g)_{max} \approx 5$. This texture was representative of the "fine grain" fraction of the microstructures produced by annealing at higher temperatures, i.e. there was no evidence of

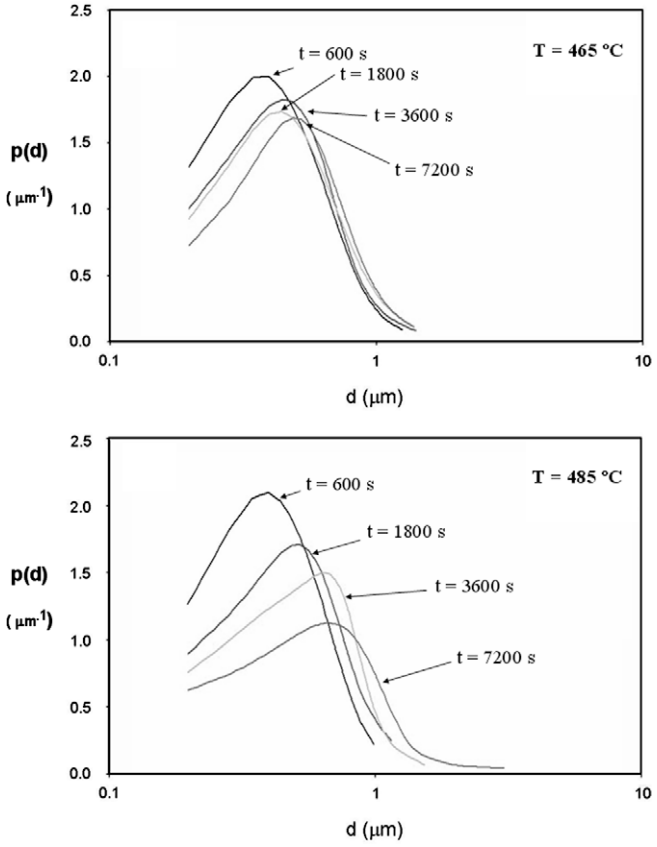


Fig. 4. Particle size distributions for material annealed at the temperatures indicated for different times, corresponding to the grain size distributions shown in Fig. 3. Particle coarsening is apparent at 485 °C, and this follows approximately the same trend as the increase in the mean matrix grain size.

texture change due to normal grain growth. Although there are inherently limited data for the textures of the abnormal grains due to the relatively small numbers that can reasonably be sampled, 33 in this research, a continuous texture can be calculated and is shown in Fig. 5b. In this case, because of the limited number of data, it is reasonable to use Gaussian smoothing with an angular width of 5° [10]. There is no significant difference between the texture characteristic of the fine-grained material and that of the abnormally large grains. The apparent rise in texture intensity can probably be ascribed to the small number of orientations. Samples of 33 orientations taken at random from the texture shown in Fig. 5a gave 5° Gaussian-spread textures with mean $f(g)_{max}$ of 15.2 with a standard deviation of 2.7. The texture shown in Fig. 5b had $f(g)_{max}$ of 19.6 and so cannot be considered as significantly different.

In the case of the island grains, it is easier to deal with the boundary misorientations, and these are better indicators of boundary anisotropy effects than the comparison of relatively weak textures. Again, the number of data is limited, 87 island grains were measured, but it is possible to produce a continuous misorientation distribution function, shown in Fig. 6. This is relatively weak, with $f(\Delta g)_{max} \approx 6.5$. This is considerably higher than the self-correlation misorientation distribution function derived from the initial fine-grained texture, with $f(\Delta g)_{max} \approx 2$, but again limited sampling means that the significance of that difference is probably very low: populations of 87 randomly chosen, uncorrelated, misorientations from the initial texture give a mean $f(\Delta g)_{max}$ of 4.3 with a standard deviation of 1.8.

### 2.4. Grain size and the spatial distribution of particles

It seems that boundary misorientation is unlikely to explain the relative stability of island grains in the present

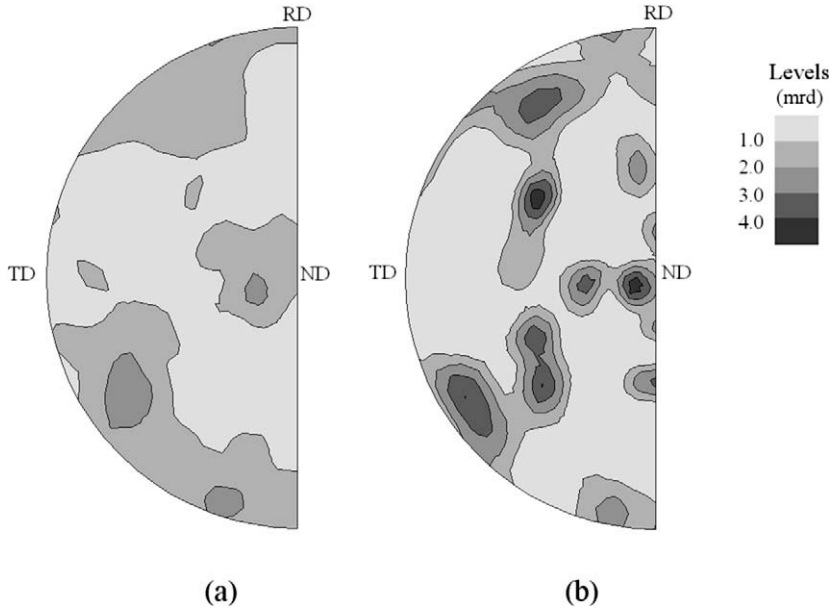


Fig. 5. Direct 0 0 1 pole figures of (a) material annealed at 400 °C for 1 h, which is representative of all the fine-grained matrix material and (b) from the orientations of abnormally large grains.

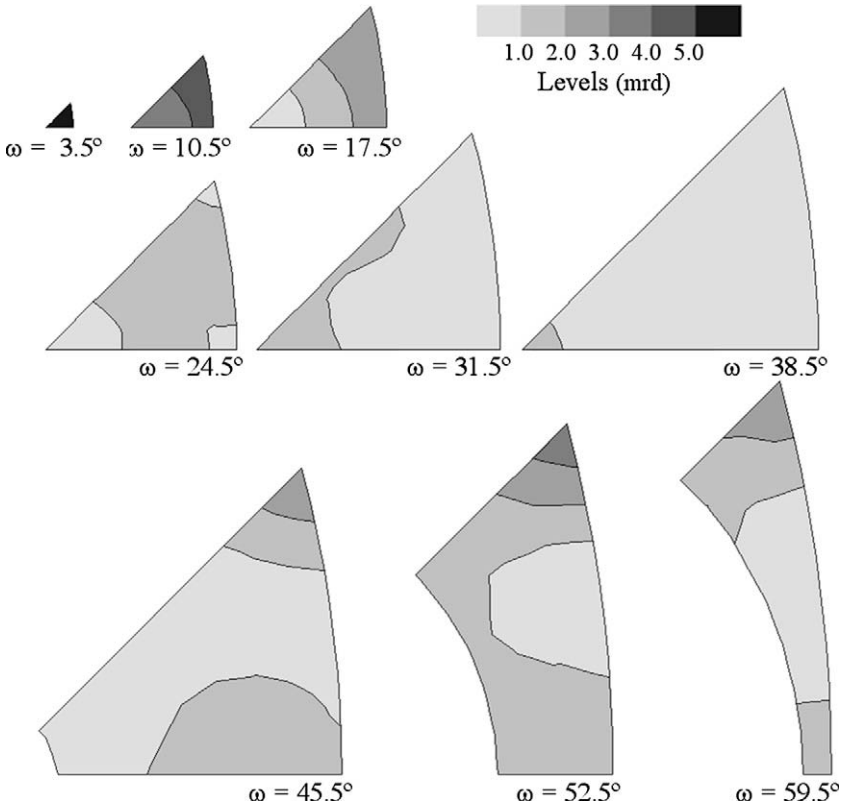


Fig. 6. Misorientation density function (MODF) of island grain boundaries. The orientation space is shown as sections through the cubic–cubic representative subspace of axis–angle measure, at constant intervals of misorientation angle, $\omega$. The size of the sections gives a volume-true representation.

material. Two further factors were considered, the island grain size and the possibility of a higher pinning pressure at the island grain boundaries. These issues were considered in a previous publication on this alloy [11]. In terms of mean section diameter, island grains were at least twice the size of the mean matrix population grains, and the conclusion drawn was that island grains had been incipient abnormal grains. In situ SEM studies backed that up, revealing that the island grains were transient features which shrank with time and so were likely to have a significant initial size advantage. In addition, some measurements of local pinning particle density were reported, and the distribution of the pinning phase in relation to the different types of grain boundaries reveals some potentially important trends.

The fraction of boundary area occupied by particles was approximated by measuring the area fraction of particles on SEM/backscattered electron images within a thin "shell" around each boundary segment. This proved convenient as part of the determination could then be done with image analysis software, and the results were judged to be a close approximation to the actual fraction of grain boundary surface taken up by $\theta$ phase, $f_A$, at least to within a constant numerical factor. Results from material annealed at 485 °C are shown in Fig. 7. All boundary fractions are higher than the volume fraction average for the material as a whole. As well as the slightly higher fraction of pinning phase at boundaries of island grains compared to boundaries in the fine-grained (matrix) parts of the microstructures, the most striking result is the relatively

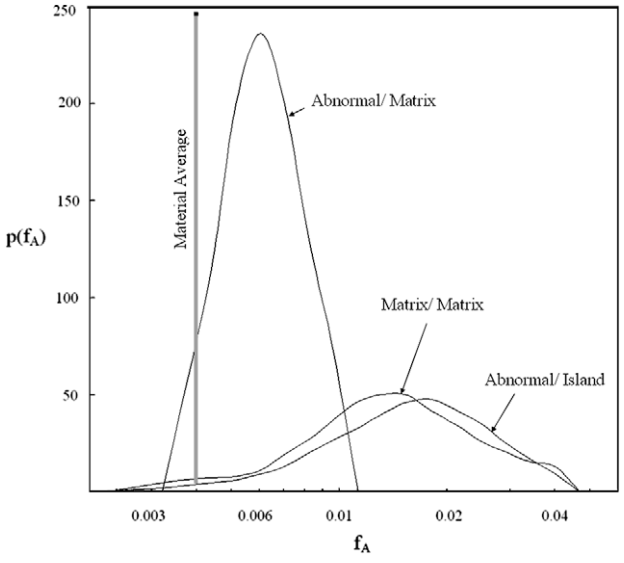


Fig. 7. Probability density functions of the volume fractions of the $CuAl_2$ pinning phase, $f_A$, located at different classes of grain boundaries in material showing abnormal growth after annealing at 485 °C for 1 h. The quantity $f_A$ will approximate closely the fraction of the grain boundary surface occupied by the pinning phase.

low fraction of pinning phase at the boundaries of the abnormal grains where they are growing into the fine-grained part of the microstructure. Those abnormal grain boundaries have about one-third of the boundary pinning phase occurring at the fine-grain material boundaries.

## 3. Discussion

It was noted in the Introduction that there is often a major focus in published work on abnormal grain growth on the effects of boundary misorientation. This is due to two factors: the practical importance of the Goss texture in silicon steels; and the fact that most processed material has a reasonably strong texture in any case. In the present work the material texture was weak and there was no significant evidence of any effect of boundary misorientation on either the growth of abnormal grains or the occurrence of island grains. In view of the strong textures that can result from abnormal grain growth, such effects cannot be ruled out but they are unlikely to be crucial for abnormal growth. At any reasonably advanced stage of growth of an abnormal grain into a nearly random matrix, any boundary anisotropy would clearly have very little effect. It could be argued that, even if the overall texture were weak, grain boundary anisotropy effects could be important on a local scale, i.e. during the early stage of abnormal growth that could be described as nucleation. However, modelling results described below indicate that "nucleation" might not be the critical stage in abnormal growth.

The grain size following ECAE and annealing was close to that predicted by the simple Zener pinning theory, assuming a random distribution of pinning particles. The $\theta$ volume fraction, $f_v$, at 400 °C was about 0.038, so with the mean particle radius of $r = 0.22$ μm, the standard formula for the limiting grain size:

$$\mathrm{Dz} = \frac{4r}{3f_v} \tag{1}$$

gives a value of about 8 μm. This is close to the measured grain size. Increasing temperature results in a decrease in $\theta$ volume fraction and, with time, an increase in particle radius as ripening occurs. At 485 °C, where abnormal growth occurred, the average volume fraction had reduced to 0.004 and even if the particle radius had not increased, Eq. (1) would predict a grain size of about 75 μm. This is considerably larger than the mean grain size of the matrix at that stage. However, as shown in Fig. 7, the content of pinning phase at matrix grain boundaries is significantly greater than the average. This is to be expected, as the free energy of particles is lower when they occupy what would otherwise be grain boundary than when they do not, and that particles at grain boundaries tend to be larger as a result of enhanced diffusion along the boundaries. The amount of pinning phase at the boundaries between the abnormal grains and the matrix grains is much closer to the average value. Zener drag per unit boundary area will depend on the fraction of grain boundary area occupied by pinning phase, $f_A$, divided by particle radius. Ignoring the particle size, and some other complicating geometrical issues, the Zener drag on the abnormal grain boundaries would typically be less than half that on the boundaries between the matrix grains. This could clearly allow a vast difference in the mobility of the abnormal grain boundaries and those between matrix grains.

The main issue following from that observation is: why is the pinning lower on the abnormal grain boundaries? It is possible that this is simply a geometric consequence of the abnormal grain boundaries migrating at a much faster speed than the matrix boundaries. There is clearly a concentration of pinning phase at the matrix grain boundaries and, to a first approximation, the faster-moving abnormal boundaries will tend to sample the volume-average pinning. It is tempting to believe that the difference in pinning is a cause, rather than simply a consequence, of abnormal growth.

The spatial correlation of pinning particles and boundaries has received attention previously. Humphreys and Hatherly [12] have reviewed the correlation effect which can occur with a random distribution of particles and dealt with correlation effects in terms of particle spacing and grain size, identifying a critical grain size above which the pinning pressure decreases to the conventional Zener value. Below that value, there is an increasing significance of pinning at grain triple junctions. However, in the present case that critical size is less than the matrix grain size. Hutchinson and Duggan [13,14] considered a situation somewhat closer to the one in the present work, where precipitation occurred on the substructural boundaries of a deformed and annealed Fe–Cu alloy. They then compared the pinning of the substructure and that of a high-angle boundary moving through the material during recrystallization. Ignoring differences in boundary surface energies, their simple analysis would predict the ratio of pinning pressure on the moving boundary to that on the matrix boundaries to be of the order of the pinning particle radius divided by the matrix grain size, i.e. D/r. In the present case, that value is very small, about 0.1 or less. Although the Hutchinson and Duggan analysis is probably in error when applied to the present work, due to assumptions about the sampling of the pinning events by the abnormal boundary, the concept is entirely consistent with that observed in the Al–Cu.

It was hoped that further insight into this matter, and a number of other issues, would be obtained via modelling. A large number of simulations using both two-dimensional vertex models [15,16] and both two- and three-dimensional MCP models [17,18] were carried out. Showing the results of all these is unfeasible here but the main summary is simply that none of them predicted abnormal grain growth. This follows most other studies when boundary anisotropy is not included.

It is generally recognized that three-dimensional modelling is required to represent the Zener pinning phenomenon [19,20]. Two-dimensional modelling is adequate to show

that grain orientation effects can easily lead to a form of abnormal growth, in which a grain surrounded by high misorientation boundary will grow rapidly into a matrix comprising grains separated by low misorientation boundaries. This is essentially because the surface energy of grain boundaries increases more rapidly with misorientation than does the mobility at low misorientations. Introducing Zener pinning into such situations was found to reduce the growth advantage of the more highly misoriented grain, and in any case this situation is not relevant to the experimental work here, where the texture was quite weak. MCP models where the pinning particles were gradually removed over time, either as complete entities or by erosion—gradual removal of particle sites in the MCP lattice—gave no real indication of abnormal growth.

In order to simplify the modelling, a number of trials were carried out with a domain which already contained a large grain. This overcomes any issues relating to the early, "nucleation" stages of abnormal growth. An example of such modelling is shown in Fig. 8. A domain of $200^3$ sites containing a volume fraction of 0.1 pinning phase sites was used to give an initial Zener-pinned structure. This is exactly the same model structure as that used previously in an investigation of dynamic grain growth [21]. The pinning particles each comprised 33 sites, sufficient to avoid the artefact of "thermal unpinning" when the high-temperature factor required to overcome lattice locking was used. A large spherical grain was created in the centre of the domain and, in the specific example shown in Fig. 8, all pinning particles not in contact with grain boundaries were removed. In this simulation, and indeed others without the intragranular particle removal, there was a period of apparent abnormal growth. However, this eventually slowed and the growth rate of the large grain reduced dramatically, as shown in Fig. 9. The abnormal growth phase appears to be transient, and the abnormal growth rate parameter used by Messina et al. [22], shown on the graph, approaches zero. In true abnormal growth, a more or less constant diametral growth rate of the abnormal grains would be expected.

One likely reason for the disparity in applying the Hutchinson and Duggan [13] analysis is that in their case the moving boundary had a higher surface energy than those of the immobile substructure. This will lead to a locally "flatter" boundary, which gives a lower sampling of the pinning phase. In the present case, the boundaries will all have rather similar energies and the abnormal boundary can adopt a less regular local geometry.

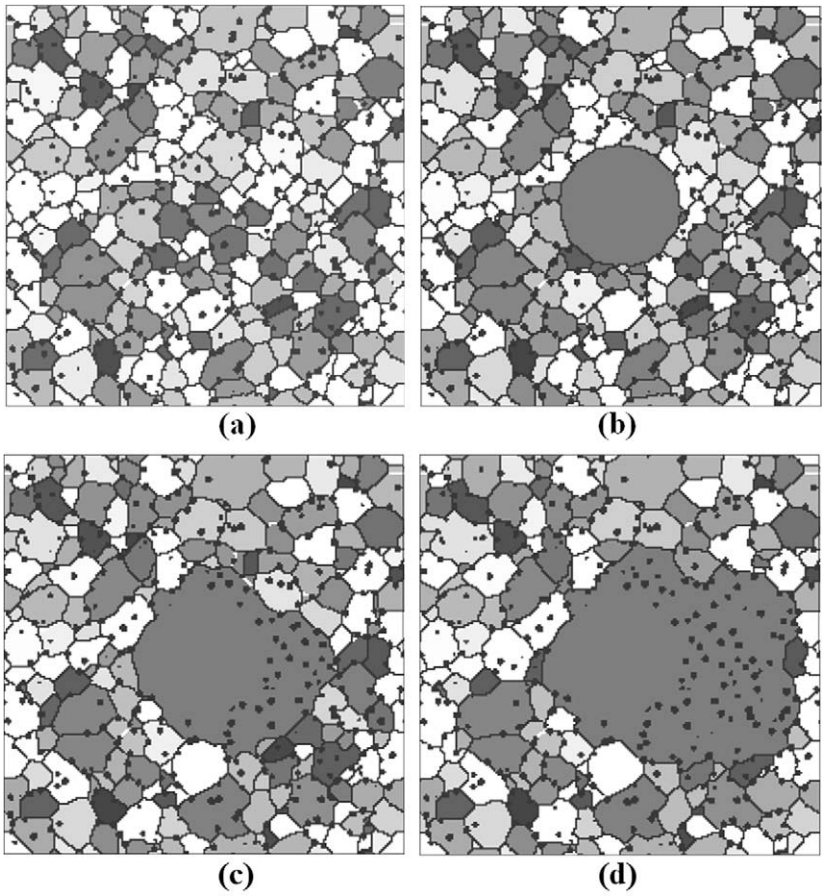


Fig. 8. Mid-plane sections through the $200^3$ domain of a MCP model. In (a), a structure close to the Zener limit is shown, into which a large grain is introduced (b) and all particles (shown in black) not in contact with grain boundaries are removed. The progress of the simulation is shown at $10^4$ μs (c) and $5 \times 10^4$ μs. (d) Superficially, abnormal grain growth is simulated but this is not actually true.

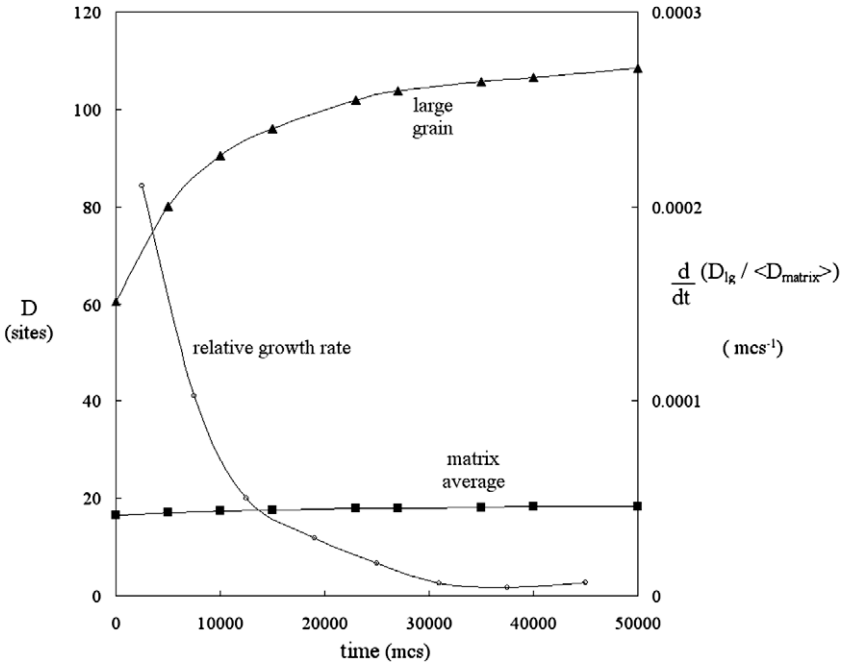


Fig. 9. The evolution of the size of the introduced large grain and the mean size of the other grains in the MCP simulation shown in Fig. 8. Although there is some "abnormal" behaviour, the growth of the large grain stagnates. This observation is reinforced by the line showing the rate of the large grain size, $D_{lg}$, normalized by the average matrix grain size, $\langle D_{\text{matrix}} \rangle$, also shown on the graph.

The volume fraction of second phase involved in the simulation shown above is significantly higher than in the experimental study. Examples of abnormal grain growth reported in published work also tend to involve quite low volume fractions of pinning phase. It may be that a geometric sampling effect of abnormal grain boundaries is dependent on there being a greater number of particles per (fine) grain than that involved in the MCP simulation. The constraints of using large particles in MCP simulations means that investigating lower volume fractions is not feasible. In order to have a reasonably large number of grains within the domain, a volume fraction of 0.01 would require a domain of about $10^9$ cells, which would mean very long simulation times. Without adequate modelling, the possibility that abnormal grain growth is caused by the boundaries of abnormal grains sampling less pinning pressure than those in the fine-grained matrix, when particle dissolution has led to the majority of the pinning phase being concentrated at the fine grain fraction boundaries, must remain as conjecture.

## 4. Conclusions

Abnormal grain growth occurs in Al–3.5 wt.% Cu, processed to give a weak crystallographic texture and equiaxed grains Zener pinned by near-spherical $CuAl_2$ particles, at temperatures of about 480 °C. Those temperatures give a pinning phase volume fraction of less than 0.01.

Because of the weak crystallographic texture, there was little possibility of special boundary misorientations being responsible for the abnormal growth, except perhaps at the early stages of such growth. There was no significant evidence of any special misorientations being associated with isolated "island" grains within abnormally large grains.

There was evidence that the fraction of pinning phase present at boundaries between the fine grains was approximately double that at the abnormal grain boundaries. The difference is thought to be due to the preferential retention of the pinning phase at nearly static boundaries. The fraction at the abnormal boundaries was only slightly higher than the volume-average phase fraction. This would represent a difference in pinning pressure which could give very large difference in boundary velocities.

Simulations using three-dimensional MCP modelling with a domain containing a pre-existing large grain in a Zener-pinned matrix failed to give abnormal growth, except for a transient effect, even when pinning particles not in contact with grain boundaries at the start of the simulation were removed. This may be due to the high volume fraction of pinning phase required in the model due to computational constraints.

## References

[1] Dunn CG, Walter JL. Secondary recrystallization. In: Margolin H, editor. Recrystallization, grain growth and textures. Metals Park (OH): ASM; 1966. p. 461.
[2] May J, Turnbull D. Trans Metall Soc AIME 1958;212:769.
[3] Hillert M. Acta Metall 1965;13:227.
[4] Andersen I, Grong Ø, Ryum N. Acta Metall Mater 1995;43:2689.
[5] Humphreys FJ. Acta Mater 1997;45:5031.
[6] Weygand D, Lépinoux J, Bréchet Y. Mater Sci Forum 2004;467–470:1123.

[7] Rollett AD, Srolovitz DJ, Anderson MP. Acta Metall 1989;37:1227.
[8] Silverman BW. Density estimation for statistics and data analysis. London: Chapman & Hall; 1986.
[9] Bunge H-J. Texture analysis in materials science. Mathematical methods. London: Butterworths; 1982.
[10] Hutchinson B, Lindh E, Bate P. In: Szpunar JA, editor. ICOTOM-12. Ottawa: NRC Research Press; 1999. p. 34.
[11] Dennis J, Bate PS, Humphreys FJ. Mater Sci Forum 2007;558–559:717.
[12] Humphreys FJ, Hatherly M. Recrystallization and related annealing phenomena. 2nd ed. Oxford: Elsevier; 2004. p. 114.
[13] Duggan BJ, Hutchinson WB. Texture development during recrystallisation and precipitation in an iron–copper alloy. In: Davies GJ, Dillamore IL, Hudd RC, Kallend JS, editors. Texture and the properties of materials (ICOTOM4). London: The Metals Society; 1976. p. 292.
[14] Hutchinson WB, Duggan BJ. Metal Sci 1978;12:372.
[15] Frost HJ, Thompson CV, Howe CL, Whang J. Scripta Metall 1988;22:65.
[16] Humphreys FJ. Mater Sci Technol 1992;8:135.
[17] Anderson MP, Srolovitz DJ, Grest GS, Sahni PS. Acta Metall 1984;32:783.
[18] Grest GS, Anderson MP, Srolovitz DJ, Rollett AD. Scripta Metall Mater 1990;24:661.
[19] Miodownik M, Martin JW, Cerezo A. Philos Mag A 1999;79:203.
[20] Miodownik M, Holm EA, Hassold GN. Scripta Mater 2000;42:1173.
[21] Bate P. The Zener pinned state: stability during hot deformation. In: Palmiere EJ, Mahouf M, Pinna C, editors. Thermomechanical processing: mechanics microstructure and control. Department of Engineering Materials, University of Sheffield: Sheffield; 2003. p. 79.
[22] Messina R, Soucail M, Kubin L. Mater Sci Eng A 2001;A308:258.